Regret and Climate Tipping Points*

Andrea Titton†

October 15, 2024

Abstract

Climate tipping points introduce abrupt, irreversible shifts in the climate system, potentially locking the world into a high-temperature regime that is difficult, if not impossible, to reverse. This paper examines the economic consequences of such tipping points, focusing on the costs associated with their unpredictability and irreversibility. Using an integrated assessment model with a climate system exhibiting positive feedback, I compute optimal abatement policies under different assumptions about the proximity of tipping points. To bound the economic cost of uncertainty surrounding the exact location of the tipping point, I compare two scenarios: one where a "wishful thinker" planner assumes the tipping point is remote and delays abatement, and another where a "prudent" planner assumes incorrectly that the tipping point is imminent. The results show that delayed action leads to significantly higher economic costs, primarily due to the need for rapid, aggressive abatement when tipping becomes imminent. Treading with caution is hence a more cost-effective policy.

*I thank my supervisors Florian Wagener and Cees Diks for the patient guidance on this paper. I also thank Rick van der Ploeg, Christoph Hambel, Frank Venmans, and Luca Taschini for the insightful discussions. Finally, I thank attendees of the EEA-ESESM conference, Rotterdam, 2024 for the constructive comments.

†CeNDEF, Faculty of Economics and Business, University of Amsterdam a.titton@uva.nl

As global temperatures rise due to greenhouse gas emissions from human activities, positive feedback mechanisms in the climate system can drive the world past critical thresholds, known as tipping points, into a regime of high temperatures. In determining optimal emission abatement policies, one trade-offs present economic gains from emissions against future climate damages from higher temperature caused by those emissions. These tipping points complicate the evaluation of optimal emission abatement policies by introducing for two major reasons. First, tipping points are hard to predict by just observing historical data (Ben-Yami et al., 2024), giving policymakers little time to react once they are detected. Second, as crossing a tipping point triggers a new hardly reversible climate regime, the resulting climate damages jump. This discontinuity implies that evaluating optimal abatement policies using marginalist analysis, such as the social cost of carbon, can lead astray.

In this paper, I study the economic costs associated with the irreversibility and unpredictability of climate tipping points. Using an integrated assessment model that incorporates positive feedback effects, I compute optimal abatement strategies under two different scenarios: one where a tipping point is imminent and another where it is remote. These scenarios are calibrated to reflect extreme cases from the climate literature (Seaver Wang et al., 2023). I then quantify the upper bound of the economic losses through two experiments. The first measures the cost incurred by a "wishful thinker" social planner who mistakenly assumes the tipping point is remote, delaying optimal abatement until after it is crossed. The second considers a "prudent" planner who incorrectly assumes the tipping point is imminent, leading to more aggressive abatement. These two scenarios provide an upper bound on the economic costs of tipping, without requiring prior assumptions about the tipping point's exact location.

I show that the costs faced by a "wishful thinker" planner are significantly higher than those faced by a "prudent" planner, highlighting that in face of uncertainty policymakers must tread with caution. However, for both planners, the costs relative to the optimal policy in a no-uncertainty scenario re-

main large, suggesting that the uncertainty around tipping points can lead to large economic losses. These losses are mostly driven by the large adjustment costs induced by "slamming the breaks" strategies, employed by the "wishful thinker" which attempts to quickly abate in case of an imminent tipping point. This analysis shows that this is a costly and ineffective policy tool. Moreover, these findings are robust across a range of societal elasticities of intertemporal substitution and relative risk aversion. Throughout the paper I compare the results to a recalibrated version of the integrated assessment model by (Hambel, Kraft and Schwartz, 2021), which serves as a benchmark. Additionally, the paper introduces a numerical solver capable of addressing large nonlinear optimization problems.

The rest of the paper is structured as follows. Section 1 puts the current paper in the context of the climate and environmental economic literature and highlights its contributions. Section 2 presents a stylised version of the model which displays the same qualitative feature: an unpredictable and irreversible tipping point. This simplified model serves as illustration of the major challenges faced in computing optimal abatement in the more general model. Section 3 introduces the climate model, the economy model, and the planner problem. Section 4 computes optimal abatement policies when tipping points are known. Section 5 introduces the "wishful thinking" and "prudent" social planner problem and computes the upper bounds on the economic cost of tipping points. Finally, section 6 concludes.

1 Related Literature

A large recent literature in economics has highlighted the importance of correctly incorporating climate dynamics when analysing the economic trade-off between emissions and climate damaged we are currently facing. The key challenge is to develop integrated assessment models that, on the one hand, are sufficiently simple to be integrated into a dynamic optimisation problem, necessary to compute the economic costs of climate change and optimal abatement

policies, and, on the other hand, are able to reproduce the key dynamics of larger, more accurate climate models. Dietz et al. (2020) show, for example, how may climate models used in economics display unrealistic lags between emissions and temperature increase and that this yields insufficiently ambitious abatement policy recommendations. Another feature of the climate dynamic that has drawn a lot of attention in economics are climate tipping points (Li, Crépin and Lindahl, 2024). These are the focus of this paper.

Early work dealing with uncertain tipping points in environmental economics (Kamien and Schwartz, 1971; Nævdal and Oppenheimer, 2007; Tsur and Zemel, 1996, among others) has modelled tipping points via jump processes. At each moment in time the state variable experiences a discontinuous jump with some probability known to the agent. This approach has been successfully employed in modelling climate tipping points by, for example, Lontzek et al. (2015), Cai, Lenton and Lontzek (2016), and Van Der Ploeg and De Zeeuw (2018). This has several advantages as it allows to readily incorporate ambiguity concerns (Lemoine and Traeger, 2016), learning (Lemoine and Traeger, 2014), and self exciting processes (Hambel, Kraft and Schwartz, 2021). Furthermore, it is analytically tractable and can be used to derive closed form approximations for the contribution of tipping points to the social cost of carbon (Li, Crépin and Lindahl, 2024; Van den Bremer and Van der Ploeg, 2021). Nevertheless, this modelling choice lacks two crucial features that are the focus of this paper. First, it does not introduce different temperature regimes and hence it is not suited to talk about the cost of reverting tipping points. Second, it still requires to define a probability distribution on the tipping event, be that real or the belief of the social planner.

Another approach is to model non-linearities in the climate explicitly. This approach, which has a long history in economics (Skiba, 1978), has been developed extensively in environmental economics (Mäler, Xepapadeas and de Zeeuw, 2003; Wagener, 2013) and specifically in climate economics (Greiner and Semmler, 2005; Nordhaus, 2019; Wagener, 2015). In this paper, I bridge these

two approaches by embedding the non-linearities in the climate dynamics into a state of the art IAM (Hambel, Kraft and Schwartz, 2021). This allows, on the one hand, to model multiple climate regimes while, on the other hand, to give reliable estimate on the costs of the tipping points.

2 Stylised Example

Before turning to the full model, this section introduces a stylised integrated assessment model with a tipping point between multiple temperature regimes. The climate component of the model employs a stylised model of positive feedbacks, compared to the full model presented in section 3.1. In addition, the planner objective is reduced to a simple optimal stopping problem. Despite this it illustrates the two main challenges tipping points introduce when computing optimal abatement. First, their unpredictability hinders evaluation of future damages. Second, their irreversibility makes analyses based on marginal emission benefits and marginal temperature damages incomplete.

Emissions of CO_2 from human economic activity E_t $[\mathrm{Gt}\,\mathrm{CO}_2]$ raise CO_2 atmospheric concentration M_t $[\mathrm{p.p.m.}]$,

$$\frac{\mathrm{d}M_t}{\mathrm{d}t} = \xi_m E_t \tag{1}$$

where ξ_m converts $\mathrm{Gt}\,\mathrm{CO}_2$ to $\mathrm{p.p.m.}$. As CO_2 is a greenhouse gas, an increase in its concentration M_t compared to pre-industrial levels M^p in turn, increases average temperature T_t $[^\circ\mathrm{C}]$. The change in temperature is given by

$$\frac{\mathrm{d}T_t}{\mathrm{d}t} = G_0 \log\left(\frac{M_t}{M^p}\right) - \lambda T_t, \tag{2}$$

where G_0 is the size of the greenhouse gas effect and λ is a stabilisation rate of

temperature[1]. In this model, temperature tends towards the steady state

$$T_t \to \frac{G_0}{\lambda} \log\left(\frac{M_t}{M^p}\right) \text{ as } t \to \infty. \tag{3}$$

Hence, as carbon concentration rises, so does the steady state temperature. Suppose, for example, that emissions E_t are constant at some level $\bar{E}$, such that CO_2 concentration grows linearly from its pre-industrial level $M_t = \bar{E}\, t + M^p$. In this case, average temperature T_t grows as illustrated in Figure 1. Consider now a

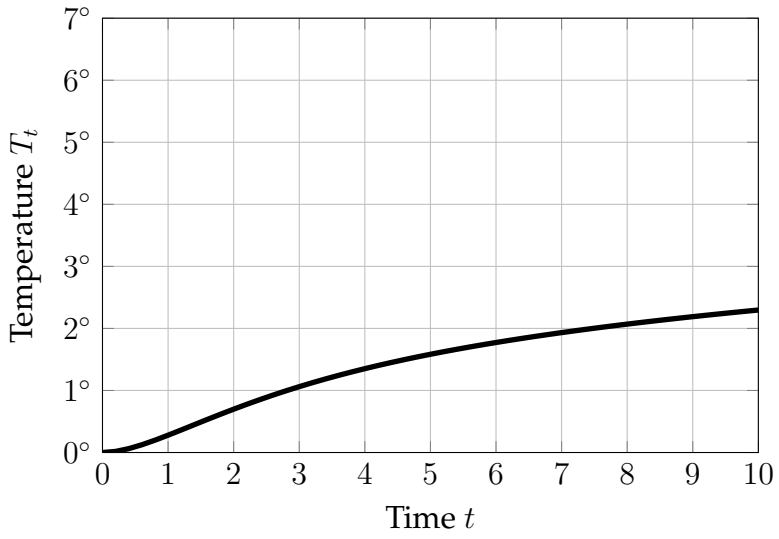

Figure 1: Path of temperatures given by (2), assuming constant emissions $E_t = \bar{E}$.

social planner who derives utility $u(E_t)$ from CO_2 emissions E_t and disutility $d(T_t)$ from temperature T_t, and discounts both at a rate ρ. For simplicity assume the emissions are constant at a level $\bar{E}$ and the social planner needs to decide at what time τ society ought to stop emitting. At that point society loses the benefits of emissions $u(\bar{E})$ and pays the damages of the resulting temperature $d(T_\tau)$. To summarise, the planner is trying to maximise

$$J(\tau) \coloneqq (1 - e^{-\rho\tau})\, u(\bar{E}) - e^{-\rho\tau}\, d(T_\tau) \tag{4}$$

by choosing an emission stopping time $\tau \geq 0$. This problem is readily solved by a marginalist planner: the optimal time τ to stop emissions is when an addi-

[1]Throughout this section, I assume for illustration purposes $G_0 = 1$, $\xi_m = 1$, and $\lambda = 1$.

tional instant of emission utility does not justify the marginal increase in temperature damages, or $\partial J/\partial \tau = 0$.

Yet, unlike the model in equation (2), the climate system is highly complex. One such complexity arises due to positive temperature feedbacks, such as ice-melting which reduces the earth's albedo or water evaporating and acting as a greenhouse gas. One way to introduce these in the toy model presented here is to assume the stabilisation rate λ to be a function of average temperature T_t[2]. In this case, the change in temperature (2) is given by

$$\frac{\mathrm{d}T_t}{\mathrm{d}t} = G_0 \log\left(\frac{M_t}{M^p}\right) - \lambda(T_t)\, T_t. \tag{6}$$

Figure 2 shows the change in temperature $\frac{\mathrm{d}T_t}{\mathrm{d}t}$ (6) as a function of temperature T_t for carbon concentration at the pre-industrial level (left panel), 50% larger (middle panel) and twice as large (right panel). As in the model without feed-

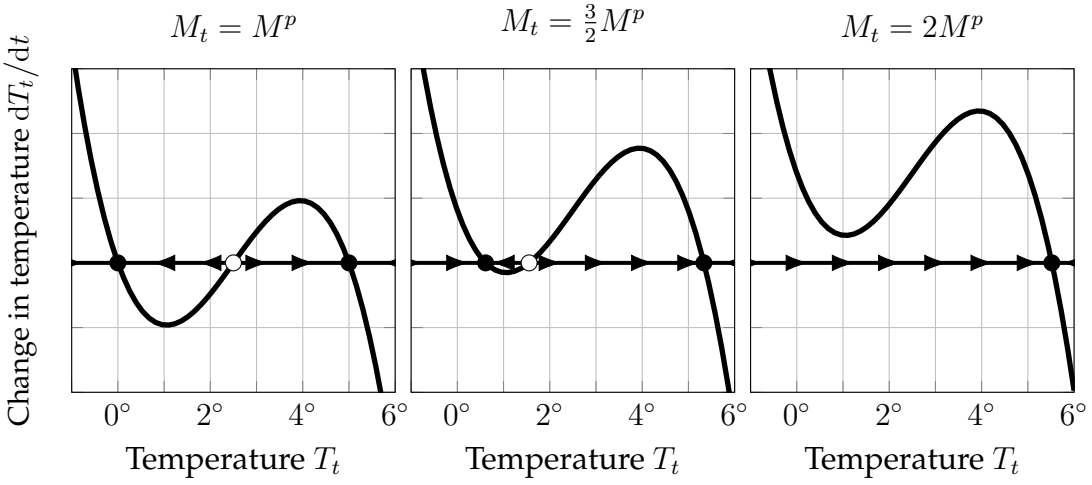

Figure 2: Change in temperature over time $\frac{\mathrm{d}T_t}{\mathrm{d}t}$ as a function of temperature T_t for three levels of atmospheric carbon concentration. The marker represents the steady state and the arrows indicate whether temperature is increasing (right) or decreasing (left).

[2]For illustration purposes, in this section I assume

$$\lambda(T_t) = aT_t^2 - 3\sqrt{\frac{c}{a}}T + 2c \tag{5}$$

where $c = 1/2$ is a scale parameter and $a = 0.08$ denotes the intensity of the feedback. Any $\lambda(T_t)$ increasing in T_t would display the same multiplicity of equilibria.

backs (2), if carbon concentration is at its pre-industrial level (left panel) there is stable level of temperature at $T_t = 0$ (left black marker). In addition to this, a new stable high temperature equilibrium is formed (right black marker). In this equilibrium, the positive feedback has trapped temperature into a high regime, for example, if all ice caps have melted the surface albedo is sufficiently high that ice is unable to form again. As carbon concentration increases (from left to right panel), the average temperature raises. Yet, unlike in the case of no feedback, the system goes through a tipping point[3]: the low temperature equilibrium becoming unfeasible triggers a sudden rise in temperature as it converges to the higher equilibrium. This phenomenon poses two problems from the point of view of the social planner trying to evaluate the trade-off between current emissions and future climate damages. First, if the temperature dynamics (6) are uncertain, one cannot hope to learn them from simply observing the path of temperature (Ben-Yami et al., 2024). To illustrate this, Figure 2 shows the path of temperature under current emissions in the presence of feedback (solid line) and in the linear case (dashed line). The two trajectories are extremely close, until the tipping point is reached. After this, they rapidly diverge. Second, marginalist calculations are not sufficient to solve the emission

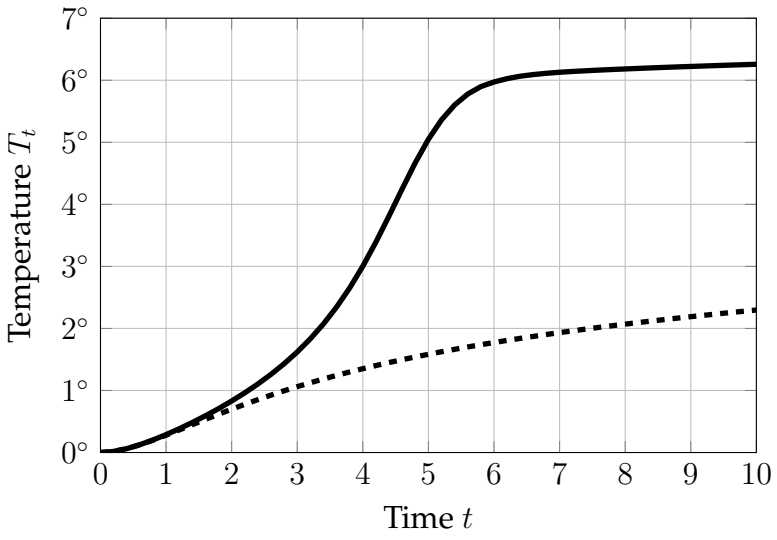

Figure 3: Path of temperatures given by (6), assuming constant emissions $E_t = \bar{E}$. The dashed line is the path without feedback as in Figure 1

[3]The system undergoes a saddle-node bifurcation.

stopping problem given in equation (4). Figure 4 shows the objective function J as a function of the stopping time. The objective is discontinuous at the tipping point because waiting an instant longer to stop emission, forces the system through a tipping point and triggers a large increase in temperature. Hence, the marginal benefits net of the marginal costs of waiting longer to stop emitting, given by $\partial J/\partial \tau$, do not carry information regarding the future tipping point.

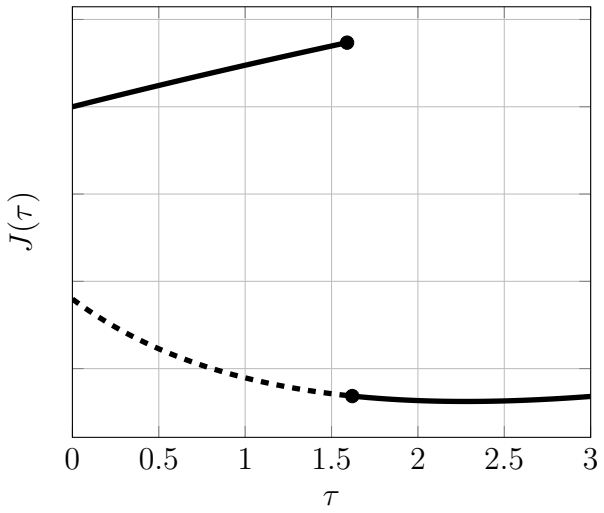

Figure 4: Objective J as a function of stopping time τ (4).

3 Model

This section extends the stylised model from section 2 by introducing a more complete climate and economy model which can be then calibrated and can produce meaningful quantitative estimates. The modelling setup and the calibration extend that of Hambel, Kraft and Schwartz (2021). The calibration of both the climate model and the economy is updated to the year 2020. Two scenarios are considered: one in which the tipping point is *imminent* and one in which it is *remote*.

3.1 Climate Model

3.1.1 CO_2 concentration and carbon sinks

Emissions from human economic activity E_t increase the average atmospheric concentration of CO_2 M_t. This, in turn, decays into natural sinks N_t. To model the saturation of natural sinks, the decay rate $\delta_m(N_t)$ falls in the quantity of carbon dioxide already stored in the natural sinks N_t. Hence, this evolves as

$$\xi_m \, \mathrm{d}N_t = \delta_m(N_t) M_t \;\; \mathrm{d}t \tag{7}$$

where ξ_m is a factor converting quantities from parts-per-million in volume to Gt of CO_2.

As we are concerned with abatement efforts, vis-à-vis a "business as usual" scenario, I rewrite variables in deviation from such scenario. Variables under business as usual are then calibrated using the IPCC SPSS5 projections (2017). Denote by E_t^b the emissions under such scenario, and by M_t^b and N_t^b the resulting carbon in the atmosphere and in natural sinks, respectively. The atmospheric concentration M_t^b under business as usual emissions evolves as

$$\frac{\mathrm{d}M_t^b}{M_t^b} = \gamma_t^b \, \mathrm{d}t + \sigma_m \, \mathrm{d}W_{m,t} \tag{8}$$

where

$$\gamma_t^b \coloneqq \xi_m \frac{E_t^b}{M_t^b} - \delta_m(N_t^b) \tag{9}$$

and $W_{m,t}$ is a Wiener process. This scenario describes an energy intensive future, in which fossil fuel usage develops rapidly and little to no abatement takes place. Using this scenario, I then calibrate the implied growth rate of carbon concentration γ_t^b. Figure 5 shows the results of the calibration (Appendix C). The upper figure shows the path of the business as usual growth rate γ_t^b and the lower figure shows the implied growth of carbon concentration M_t^b. The carbon concentration in this scenario is assumed to grow at an increasingly fast rate until 2080, when the growth rate peaks at around 1.4%. Thereafter, the

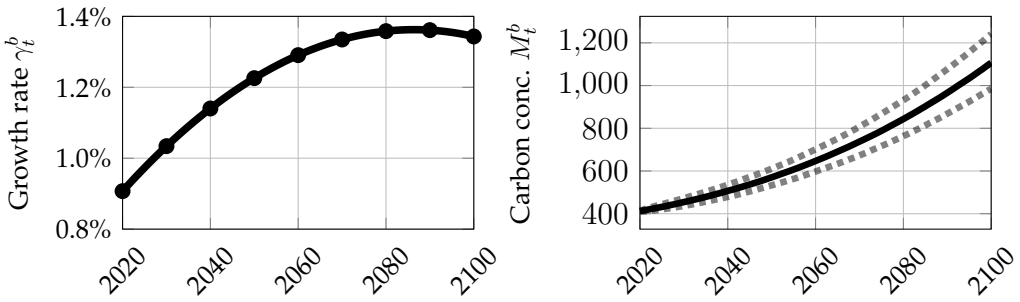

Figure 5: Growth rate of carbon concentration in the business as usual scenario γ_t^b and median path (solid) of business as usual carbon concentration M_t^b (8) with 95% simulation interval (dashed).

growth rate starts declining. The growth rate of carbon concentration γ_t^b M_t^b is always positive, hence in the business as usual scenario, carbon concentration is always increasing.

Abatement efforts α_t lower the growth rate of carbon concentration M_t vis-à-vis the business as usual scenario M_t^b. That is, the growth rate of carbon concentration M_t satisfies

$$\frac{\mathrm{d}M_t}{M_t} = \left(\gamma_t^b - \alpha_t\right)\mathrm{d}t + \sigma_m\,\mathrm{d}W_{m,t} \tag{10}$$

where $\mathrm{d}W_{m,t}$ is a Wiener process.

Not implementing any abatement policy $\alpha_t = 0$ corresponds to a business as usual scenario $M_t \equiv M_t^b$, while implementing a full abatement policy $\alpha_t = \gamma_t^b$ stabilises carbon concentration. Any abatement policy α_t can be implicitly linked back to the corresponding level of emissions by introducing an emission reduction rate $\varepsilon(\alpha_t)$, which keeps tracks of what percentage of emission has been abated

$$E_t = \left(1 - \varepsilon(\alpha_t)\right)E_t^b. \tag{11}$$

In this paper I assume that the planner does not have access to carbon capture technology. This is implemented by imposing that abatement cannot exceed the growth rate of carbon concentration and the carbon decay into natural sinks, namely

$$\alpha_t \leq \gamma_t^b + \delta_m(N_t). \tag{12}$$

3.1.2 Temperature

Earth's radiating balance, in its simplest form, prescribes that an equilibrium temperature $\bar{T}$ is determined by equating incoming solar radiation S with outgoing long-wave radiations $\eta\sigma\bar{T}^4$, where σ is the Stefan-Boltzmann constant and η is an emissivity rate. Due to the presence of greenhouse gasses, certain wavelengths are scattered and, hence, not emitted[4]. This introduces an additional radiative forcing G which yields the balance equation $S = \eta\sigma\bar{T}^4 - G$. Focusing on the role of increased CO_2, as opposed to other greenhouse gases, we can decompose the greenhouse radiative forcing term G into a constant component G_0 and a component which depends on the steady state level of CO_2 concentration in the atmosphere M_t with respect to the pre-industrial level M^p, such that

$$G \equiv G_0 + G_1 \log(M_t/M^p). \tag{13}$$

I introduce a feedback in the temperature by assuming that the absorbed incoming solar radiation is increasing in temperature. This choice can be seen as a stylised model of the ice-albedo feedback (Ashwin et al., 2012; McGuffie and Henderson-Sellers, 2014), yet, any positive feedback in temperature dynamics yields a similar interpretation. Similarly, incoming solar radiation S can be decomposed as $S_0\,(1 - \lambda(T_t))$ where the function $\lambda(T_t)$ transitions from a higher λ_1 to a lower level $\lambda_1 - \Delta\lambda$ via a smooth transition function $L(T_t)$. To control at which level of temperature the transition occurs the transition functions take the form

$$\lambda(T_t) \coloneqq \lambda_1 - \Delta\lambda\big(1 - L(T_t)\big) \text{ with} \tag{14a}$$

$$L(T_t) \coloneqq \frac{1}{1 + \exp\left(-L_1\left(T_t - T^c\right)\right)} \tag{14b}$$

where T^c is the level of temperature at which the feedback effect begins and L_1 is a speed parameter.

The costs that society incurs if it behaves under the wrong assumption over

[4]See Ghil and Childress (2012) for a more detailed discussion.

T^c are the focus of the subsequent sections. Best estimates from climate sciences are that many such transitions occur for average global temperatures between $1.5°$ and $3°$ over pre-industrial levels (Seaver Wang et al., 2023). A large body of literature has focused on estimating critical thresholds associated with climate tipping (e.g. Boulton, Allison and Lenton 2014; Van Westen, Kliphuis and Dijkstra 2024), yet for many such tipping points either the uncertainty is too large (Ben-Yami et al., 2024) or it is not theoretically possible to do so (Ditlevsen and Johnsen, 2010; Wagener, 2013). To avoid attaching an arbitrary prior over such threshold, in this paper I choose to focus on two extreme scenarios: one in which the tipping point is *imminent* $T^c = 1.5°$ and one in which it is *remote* $T^c = 2.5°$. The parameter $\Delta\lambda$ is calibrated by matching the climate sensitivity, that is, the expected equilibrium temperature of doubling CO_2 concentration $M_t = 2M^p$, of $4.5°$, which is the upper end of the range deemed very likely in AR6 (IPCC, 2023). Figure 6 shows the transition function (14) under these two scenarios. Despite being a highly stylised and reduced form representation of

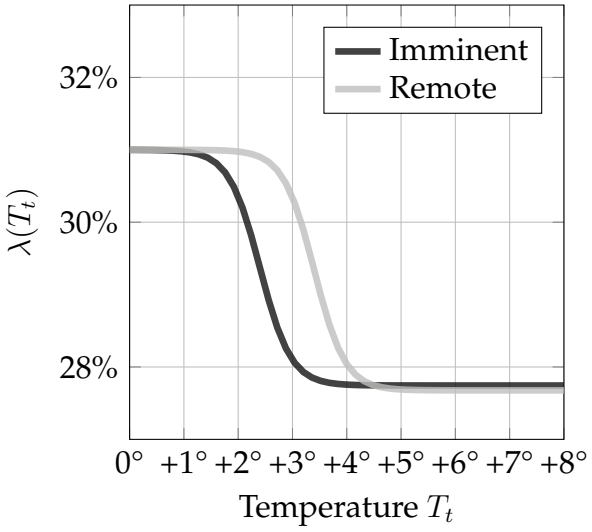

Figure 6: Coefficient $\lambda(T)$ for different threshold temperatures $T^c \in \{1.5, 3.5\}$

a complex and spatially heterogeneous process, λ captures the core mechanism behind feedback processes in the temperature dynamics that can generate tipping points (McGuffie and Henderson-Sellers, 2014). These simple feedback dynamics allow us to discuss and estimate the costs of ending in a new regime,

what ought to be done to prevent this from happening or not, and the regret associated with their uncertainty.

Putting these processes together we can write the two determinants of temperature dynamics: radiative forcing, which only depends on temperature,

$$r(T_t) \coloneqq S_0 \left(1 - \lambda(T_t)\right) - \eta\sigma T_t^4 \tag{15}$$

and the greenhouse gas effect, which only depends on atmospheric carbon concentration

$$g(M_t) \coloneqq G_0 + G_1 \log(M_t/M^p). \tag{16}$$

Under these two drivers, temperature changes are given by

$$\epsilon \, \mathrm{d}T_t = r(T_t) \, \mathrm{d}t + g(M_t) \, \mathrm{d}t + \sigma_T \, dW_{T,t}, \tag{17}$$

where ϵ is the thermal inertia and $W_{T,t}$ is a Wiener process.

3.1.3 Tipping Points

The presence of the feedback effect λ introduces tipping points in the temperature dynamics. This is illustrated in Figure 7. For a given level of carbon concentration $\bar{M}$, the temperature $\bar{T}$ tends towards radiative balance $r(\bar{T}) = -g(\bar{M})$ (solid line). For low values of carbon concentration $\bar{M} \lesssim 350$, such steady state is unique. As more carbon dioxide gets added to the atmosphere, two additional steady state levels of temperature $\bar{T}$ arise, one stable (upper solid line) and one separating unstable (dashed line). The presence of the additional steady state is hard to detect as the relationship between temperature T_t and carbon concentration M_t remains approximately log-linear. This makes estimating the presence of a tipping point and its threshold T^c unfeasible using purely historical data. As carbon concentration increases further $M_t \gtrsim 490$ and temperature crosses the critical threshold T^c, the old stable and low temperature regime is no longer feasible and only a high stable temperature regime remains. Any increase of carbon concentration at this tipping point then leads

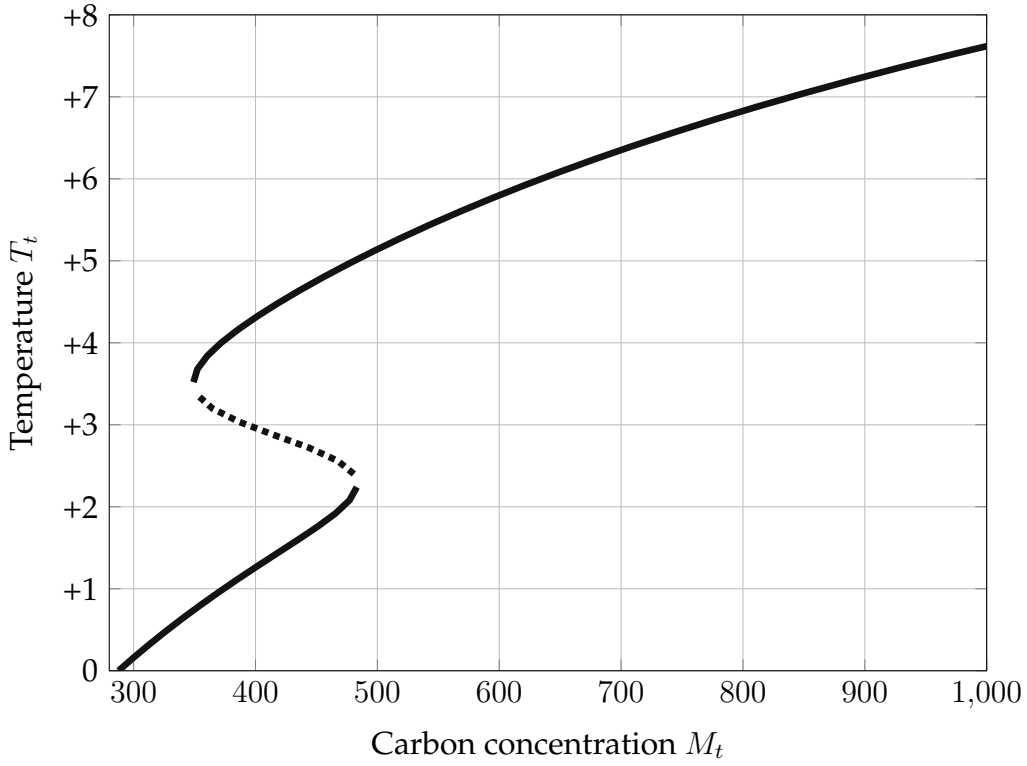

Figure 7: Steady states of temperature T_t and carbon concentration M_t for $T^c = 2°$. The solid and dashed lines represent attracting and repelling steady states, respectively.

to a rapid increase in temperature to a this new steady state. Crucially, to revert the system back to the lower temperature regime, it is not sufficient to remove just the carbon that caused the system to tip, but society would have to remove all carbon until the only stable steady state is the low temperature, hence back to $M_t \lesssim 350$ ("walking along" the upper solid line). In the context of the example of an ice-albedo tipping point, at low level of carbon concentration the Earth's ice coverage is large and the albedo coefficient, that is, the percentage of solar radiation reflected by the lighter coloured surface. As temperature rises, and ice melts, the albedo decreases, which further contributes to temperature increases. This positive feedback might push the world into an "ice-free" regime with low albedo. To restore ice coverage temperature must decrease further than the increase of the tipping point.

Figure 8 displays how this mechanism impacts the dynamics of temperature under the business as usual scenario for an imminent tipping point, $T^c = 1.5°$ (darker), and a remote one, $T^c = 2.5°$ (lighter). The lines with the markers

show a simulation of temperature T_t (17) and carbon concentration M_t under business as usual (8). Markers denotes the temperature and carbon concentration every 10 years starting from 2020. For the first two decades, the temperature dynamics are identical. Then, if the tipping point is imminent $T^c = 1.5°$, suddenly temperature grows rapidly to the new steady state and the system converges to a higher temperature regime, before the log-linear relationship between temperature T_t and carbon concentration M_t is established again. This occurs much later whenever the critical temperature T^c is higher and, hence, the tipping point is remote.

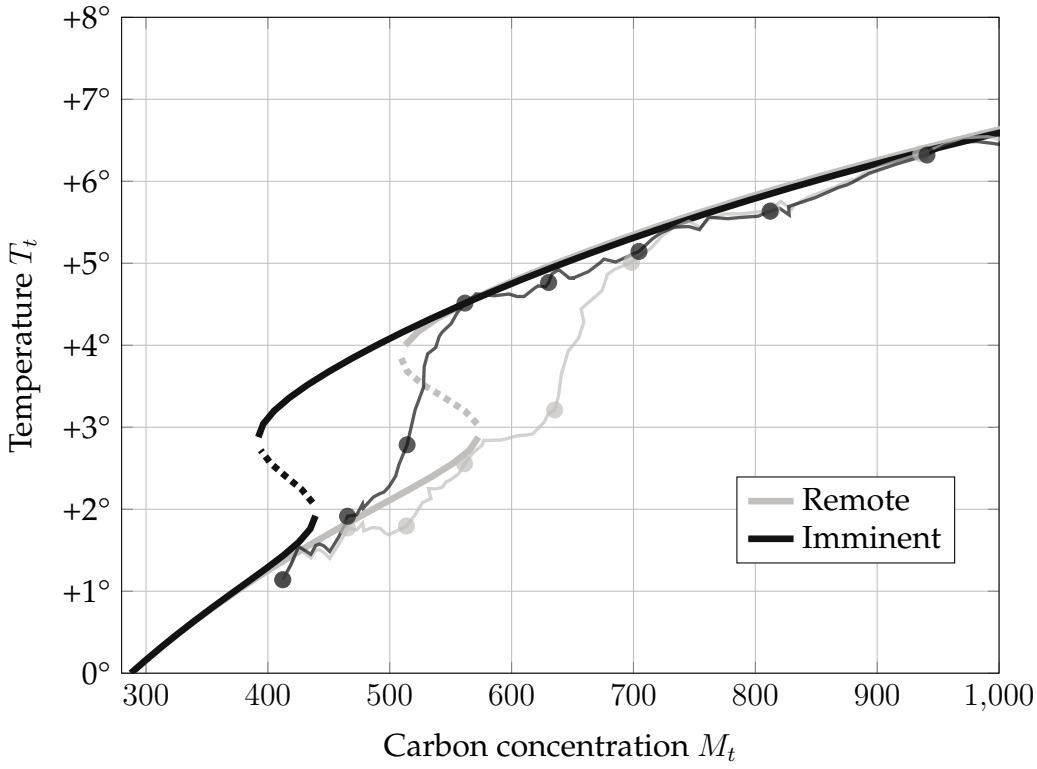

Figure 8: Steady states of temperature T_t and carbon concentration M_t for $T^c = 1.5°$ (dark) and $T^c = 2.5°$ (light). The solid and dashed lines represent attracting and repelling steady states, respectively. The marked line show two simulation of temperature and carbon concentration under the business as usual scenario. Markers denotes the temperature and carbon concentration every 10 years starting from 2020.

3.1.4 Differences with the Benchmark Model

Previous literature in climate economics has, in large part, modelled tipping points by assuming that, at each moment in time, with some instantaneous

probabilities $\pi(T_t)$ there is a temperature shock of size $q(T_t)$, both of which are increasing in temperature (e.g. Hambel, Kraft and Schwartz 2021; Lemoine and Traeger 2016; Van Der Ploeg and De Zeeuw 2018). This approach is also known as state-distributed catastrophe (Li, Crépin and Lindahl, 2024). Formally, under this assumption, equation (17) is modified into

$$\epsilon \, \mathrm{d}T_t = r_l(T_t) \, \mathrm{d}t + g(M_t) \, \mathrm{d}t + \sigma_T \, \mathrm{d}W_{T,t} + q(T_t) \, \mathrm{d}N_t \, (T_t) \tag{18}$$

where N_t is a Poisson process with arrival rate $\pi(T_t)$ and r_l, unlike r (15), is linear. This choice captures a key feature of tipping points: as carbon concentration rises, we expect warmer shocks to be more persistent and hence the steady state temperature distribution to be skewed (IPCC, 2023; Weitzman, 2014). Furthermore, the shock arrival rate π and its size q can be easily calibrated. Yet, as it does not allow for multiple temperature regimes, it is not suited to answer questions on the costs of tipping and the potential regret associated with tipping points. Hence, in this paper I consider the tipping point formulation given in (17), which generates multiple temperature regimes whilst still producing skewed steady state temperature distributions. An illustration of this is given in the comparison Figure 9.

3.2 Economy

This section introduces the economy and its feedbacks with the climate. In line with the literature (e.g. Barro 2006; Hambel, Kraft and Schwartz 2021; Pindyck and Wang 2013), I assume an Harrod–Domar model of the economy.

3.2.1 Capital Accumulation and Climate Damages

Output

$$Y_t = A_t K_t. \tag{19}$$

is the product of the capital stock K_t and its productivity A_t. The latter grows at a constant rate ϱ. Output Y_t can be used for investment in capital I_t, abate-

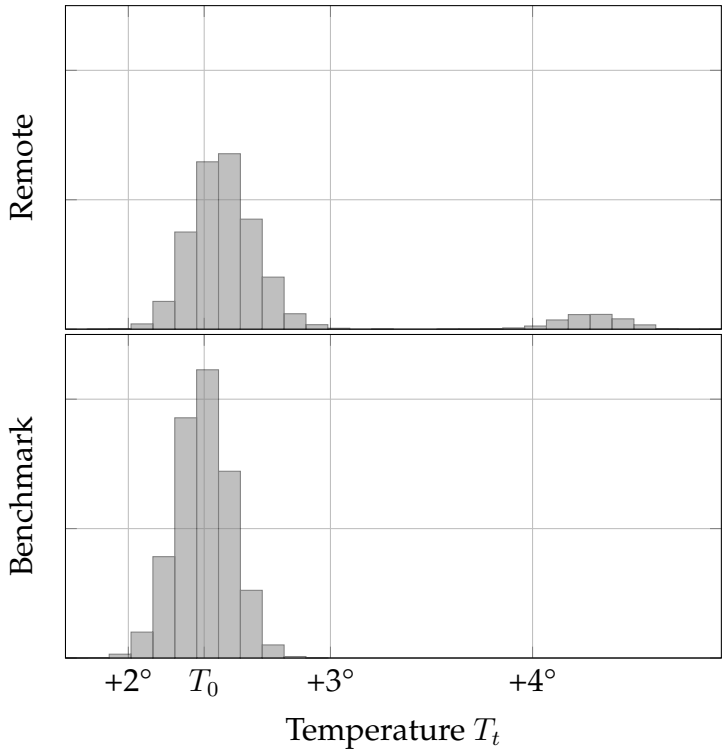

Figure 9: Distribution of temperature T_t obtained from simulation dT_t from (17) and (18) (benchmark) for 1000 years at a constant carbon concentration level $M = 540$ p.p.m. starting at T_0.

ment expenditures B_t, or consumption C_t. This implies the nominal budget constraint

$$Y_t = I_t + B_t + C_t. \tag{20}$$

Capital K_t depreciates at a rate δ_k but can be substituted by capital investments I_t, which incurs, along with abatement expenditure B_t, in quadratic adjustment costs

$$\frac{\kappa}{2}\left(\frac{I_t + B_t}{K_t}\right)^2 K_t. \tag{21}$$

Climate change interacts with the economy by lowering capital growth via damages $d(T_t)$ which are increasing in temperature T_t. Following Weitzman (2012), I assume the damage function to take the form

$$d(T_t) := \xi\, T_t^v. \tag{22}$$

The calibrated damage function is displayed in Figure 10. This stylised form

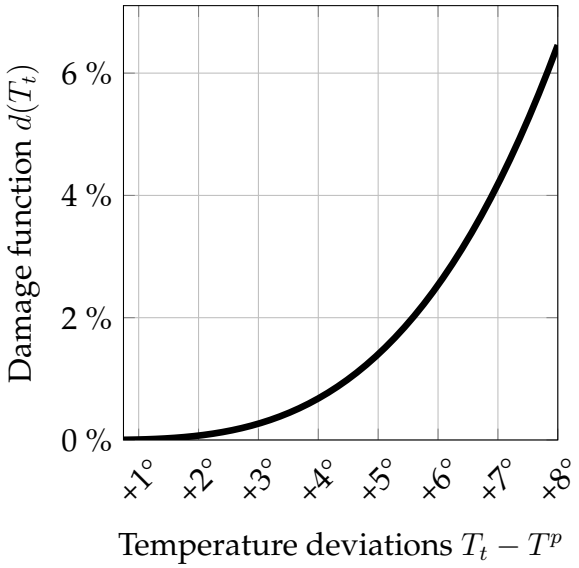

Figure 10: Damage function with the Weitzman (2012) calibration.

captures the empirical evidence that under higher temperature levels some forms of capital, particularly in the agricultural (Dietz and Lanz, 2019) or manufacturing sectors (Dell, Jones and Olken, 2009, 2012), become more expensive or harder to substitute. A common alternative in the literature is to assume that higher temperatures wipe out part of the capital stocks (Nordhaus, 1992). The comparison between these two assumption is carried out in Appendix **??** and a thorough treatment can be found in Hambel, Kraft and Schwartz (2021).

Combining the endogenous growth of capital and the climate damages, the growth rate of capital satisfies

$$\frac{\mathrm{d}K_t}{K_t} = \left(\frac{I_t}{K_t} - \delta_k - \frac{\kappa}{2} \left(\frac{I_t + B_t}{K_t} \right)^2 \right) \mathrm{d}t - d(T_t)\,\mathrm{d}t + \sigma_k\,\mathrm{d}W_k\,, \tag{23}$$

where W_k is a Wiener process.

In the following, I link the abatement costs B_t with the abatement rate α_t, introduced in the previous section. Introduce $\beta_t \coloneqq B_t/Y_t$ the fraction of output devoted to abatement. I assume this to be quadratic function of the fraction of abated emissions $\varepsilon(\alpha_t)$ (11), namely,

$$\beta_t(\varepsilon(\alpha_t)) = \frac{\omega_t}{2}\,\varepsilon(\alpha_t)^2. \tag{24}$$

Under this assumption, no abatement is free, as $\beta_t(0) = 0$. At a fixed time t, an higher abatement rate α_t and hence an higher emission reduction $\varepsilon(\alpha_t)$ vis-à-vis the business as usual scenario, becomes increasingly costly at linear rate $\omega_t\varepsilon(\alpha_t)$. It is common in the literature to assume the marginal abatement costs to be proportional to output and linear in abatement efforts (Baker, Clarke and Shittu, 2008; Dietz and Venmans, 2019; Nordhaus, 1992, 2017). As noted by Dietz and Venmans (2019, p.112-113), the proportionality with output arises because higher output growth increases energy demand. This must be satisfied with low-carbon energy technology which display decreasing marginal productivity. The linearity in abatement efforts is assumed as it matches the empirical estimates provided in the IPCC Fifth Assessment Report (2023).

As time progresses, so does abatement technology and a given abatement objective becomes cheaper, as a fraction of output. This is modelled by letting the exogenous technological parameter ω_t decrease exponentially over time

$$\omega_t = \omega_0 e^{-\omega_r t}. \tag{25}$$

Following (Nordhaus, 2017), I assume that full abatement $\varepsilon(\alpha_t) = 1$ costs 11% of GDP in 2020 and 2.7% of GDP in 2100. These estimates are in line with a large literature estimating marginal abatement curves (see the meta-analysis by Kuik, Brander and Tol 2009). The resulting marginal abatement curves are displayed in Figure 11.

Finally, let

$$\chi_t \coloneqq \frac{C_t}{Y_t} \tag{26}$$

be the fraction of output devoted to consumption. Using the budget constraint (20) and the two controlled rates, the abatement efforts α_t and the consumption rate χ_t, the growth rate of capital (23) can be rewritten as

$$\frac{\mathrm{d}K_t}{K_t} = \Big(\phi_t(\chi_t) - A_t\beta_t(\varepsilon(\alpha_t)) - d(T_t)\Big)\,\mathrm{d}t + \sigma_k\,\mathrm{d}W_{k,t} \tag{27}$$

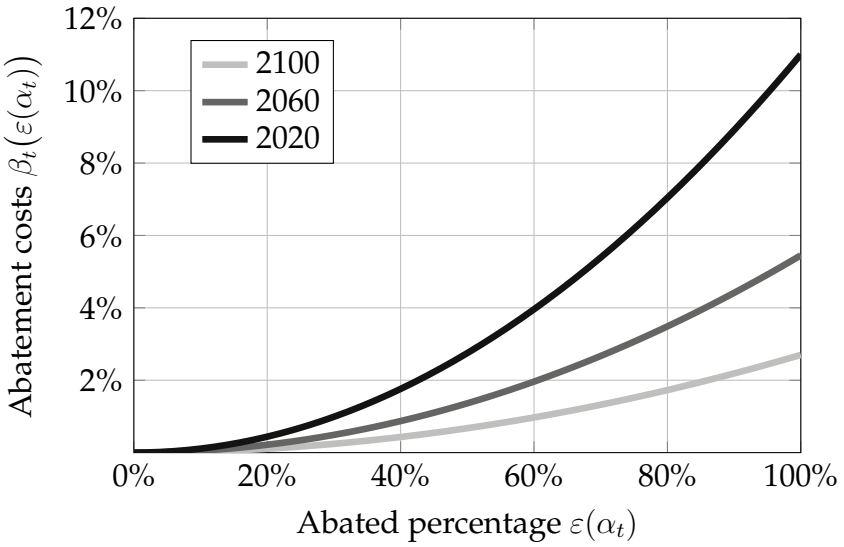

Figure 11: Calibrated marginal abatement curves $\beta_t'(\varepsilon) = \omega_t \varepsilon$ at different times t.

where

$$\phi_t(\chi_t) \coloneqq A_t(1-\chi_t) - \frac{\kappa}{2} A_t^2 (1-\chi_t)^2 - \delta_k \tag{28}$$

is an endogenous growth component, $\beta_t(\varepsilon(\alpha_t))$ is the fraction of output allocated to abatement for an abatement rate α_t, and $d(T_t)$ are the damages from climate change. This formulation makes the trade-off between climate abatement and economic growth apparent. Devoting fewer resources to abatement to pursue higher capital growth, and hence, output growth, yields higher future temperature and can put the economy in a lower growth path altogether.

Finally, as output Y_t is just the product of capital K_t and productivity A_t, its growth rate differs from that of capital just by the growth rate of productivity

$$\frac{\mathrm{d}Y_t}{Y_t} = \varrho + \frac{\mathrm{d}K_t}{K_t}. \tag{29}$$

4 Optimal Abatement

Given the climate and economic dynamics described in the previous section, in the following I introduce the objective of the social planner and the resulting maximisation problem. At time t given the state of temperature, carbon concentration, carbon in sinks, and output $X_t \coloneqq (T_t, M_t, N_t, Y_t)$, societal utility is

recursively defined as

$$V_t(X_t) = \sup_{\chi,\alpha} \mathbb{E}_t \int_t^\infty f(\chi_s(X_s)Y_s, V_s(X_s))\,\mathrm{d}s \tag{30}$$

where χ and α are continuous policies over time and the state space, and f is the Epstein-Zin aggregator

$$f(C,V) \coloneqq \rho \frac{(1-\theta)\,V}{1-1/\psi}\left(\left(\frac{C}{((1-\theta)V)^{\frac{1}{1-\theta}}}\right)^{1-1/\psi} - 1\right). \tag{31}$$

Consumption is integrated into a utility index by means of the Epstein-Zin integrator (Duffie and Epstein, 1992). This aggregator plays a dual role. First, it allows to disentangle the role of relative risk aversion θ, elasticity of intertemporal substitution ψ, and the discount rate ρ in determining optimal abatement paths. Second, it circumvents the known paradoxical result that abatement policies becomes less ambitious as society becomes more risk averse (Pindyck and Wang, 2013). The baseline model presented below assumes $\rho = 1.5\%$, $\theta = 10$ and $\psi = 0.75$, as in Hambel, Kraft and Schwartz (2021). Details on the numerical solution of problem (30) are given in Appendix B.

As mentioned above, we consider two possible dynamics for temperature T_t. One with an imminent and one with a remote tipping point. Let $\underline{\alpha}_t$ and $\overline{\alpha}_t$ be the optimal abatement in case of an imminent and a remote tipping point respectively. Figure 12 shows how optimal policies behaves in a regime with tipping points. Each panel shows the fraction of abated emissions ε_t compared to the business as usual in the imminent (left) and remote (right) tipping point, as a function of the current carbon concentration M_t. As the tipping point generates multiple temperature regimes for a given carbon concentration level M_t, each panel shows two figures. The lighter curve represents the abatement undertook before tipping, in a low temperature regime. The darker curve represents the policy after tipping, in a high temperature regime. The optimal policy is hence not unique and switches in the event of tipping. In case of an imminent tipping point (left panel), while in a low temperature regime (lighter curve),

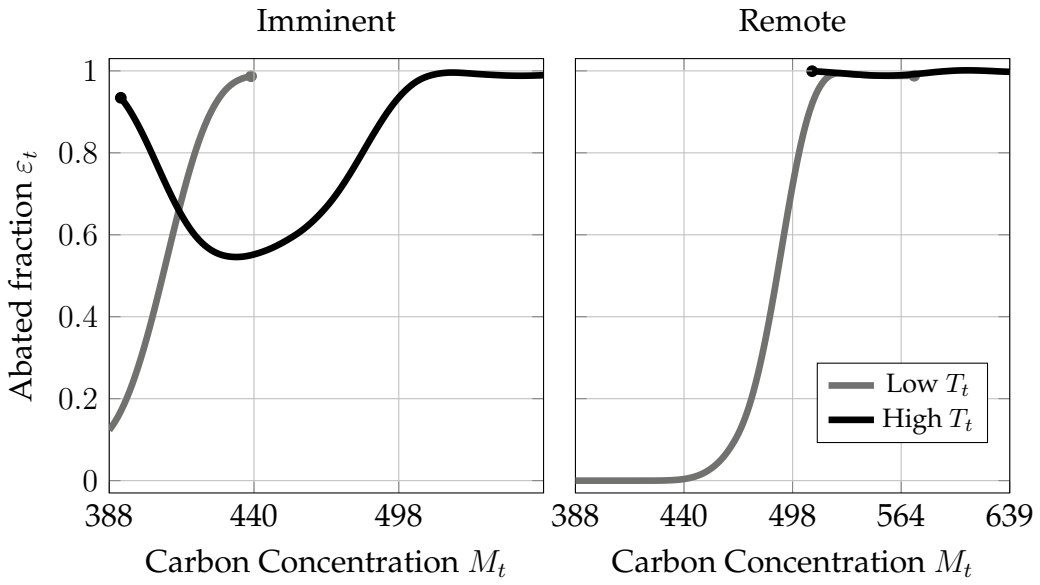

Figure 12: Fraction of abated emissions ε_t at different levels of carbon concentration M_t, for an imminent (left panel) and remote (right panel) point. To aid illustration, all other dimensions (T_t, N_t, Y_t) are set to their steady state value. As for some values of M_t there are two steady states of temperature T_t, two curves are shown.

the fraction of abated emission ε_t increases rapidly to 1 as carbon concentration rises. If the tipping point is crossed and the climate system switches to a high temperature regime abatement efforts are scaled back (darker curve) as the climate is irreversibly in a regime of high temperature. This results underpins a strong policy result: crossing a tipping point immediately weakens abatement incentives, hence, it is optimal to rapidly scale up abatement before that happens. Finally, notice that, if the climate has tipped but carbon concentration is low, it is still worth abating a large fraction of emissions (u-shaped dark curve) because a random negative shock in temperature can push the system back to a low-temperature regime. At the other extreme, if the tipping point is remote (right panel) it does not affect optimal policy. Abatement efforts are increasing in carbon concentration and full abatement is reached, in both regimes, at around 500 p.p.m..

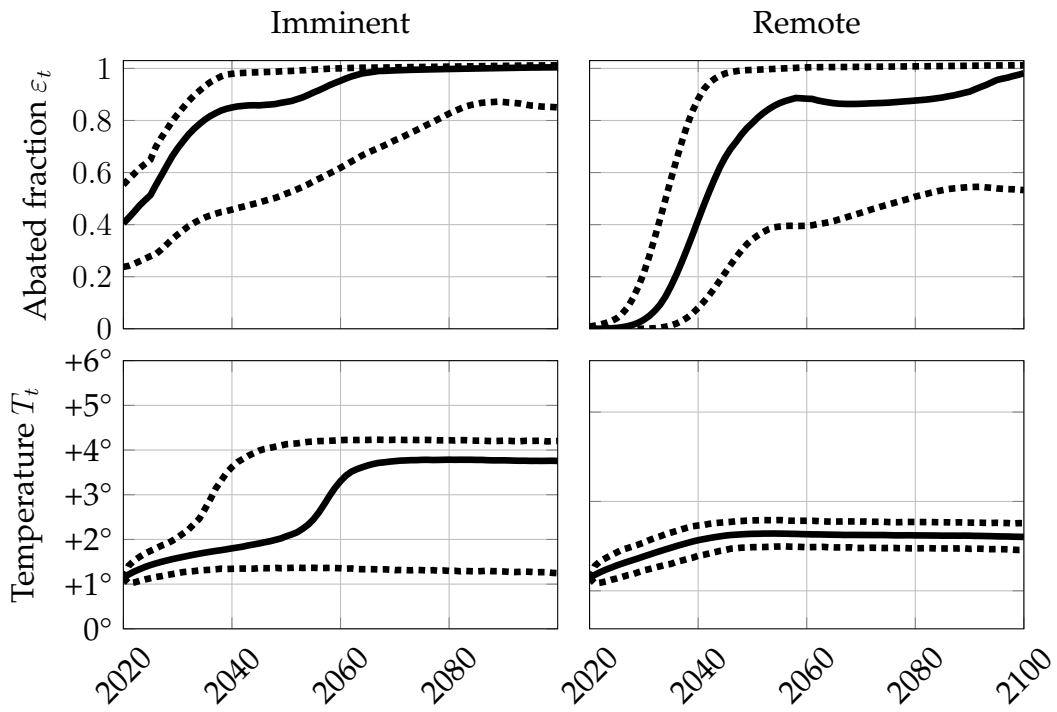

Figure 13: Median (solid line) and 95% simulation intervals (dotted line) of abated fraction ε_t and temperature T_t under optimal policies in the imminent and remote scenarios. 10000 simulations.

These policies, when implemented, yield a path of temperature and, as a consequence, temperature damages. Figure 13 shows the median path of the abated fraction of emission ε_t (solid line) and the resulting temperature path T_t with 95% simulation intervals (dotted lines), for an imminent (left panel) and a remote (right panel) tipping point. As expected, in case of an imminent tipping point, abatement is promptly ramped up. In the median case 40 % of the business-as-usual emissions are abated immediately. Thereafter, abatement ramps up and net-zero is attained by 2060. These large efforts are not sufficient to completely prevent tipping as by 2040 the climate system has tipped with 5% probability and by 2060 with 50% probability. In case the tipping point is remote, the planner has more time to postpone abatement, which is cheaper in the future, and is able to stabilise temperature at around 2° without tipping.

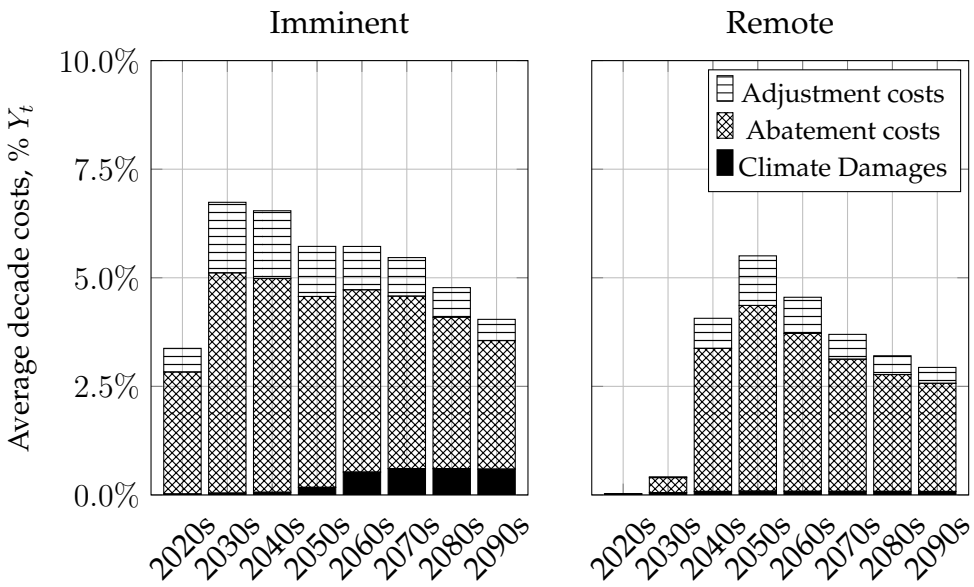

Figure 14

5 Wishful Thinking and Prudence

The previous section discussed the optimal policies of a planner that knows whether the tipping point is imminent or remote. This section tackles the unpredictability of the tipping points (Ben-Yami et al., 2024). Consider first a "wishful thinker" planner who abates under the assumption that the tipping point is remote, while it is in fact imminent. I assume that at the time the positive feedback in the climate system is triggered

$$\tau \coloneqq \inf_t \{T_t \geq T^c \equiv 1.5^\circ\} \tag{32}$$

the planner recognises their mistakes and switches to the optimal strategies. The abatement policy of the wishful thinker planner (w) is then given by

$$\alpha_t^w = \begin{cases} \overline{\alpha}_t & \text{if } t < \tau, \\ \underline{\alpha}_t & \text{if } t \geq \tau. \end{cases} \tag{33}$$

Figure 15 shows the path of the abated fraction of emissions ε_t (top left panel), the resulting expenditure in abatement as a % of output Y_t (top right panel), the temperature T_t (bottom left panel), and the carbon concentration (bottom right panel). As the expected, the planner begins by postponing abatement efforts ($\varepsilon_t = 0$) before "slamming the break" a decade down the line, when the feedback loop is triggered. This strategy requires a rapid rump-up of abatement expenditures which peak at 6% of output. Despite the quick abatement rump-up, by 2050 the climate is in a high temperature regime with 95% probability.

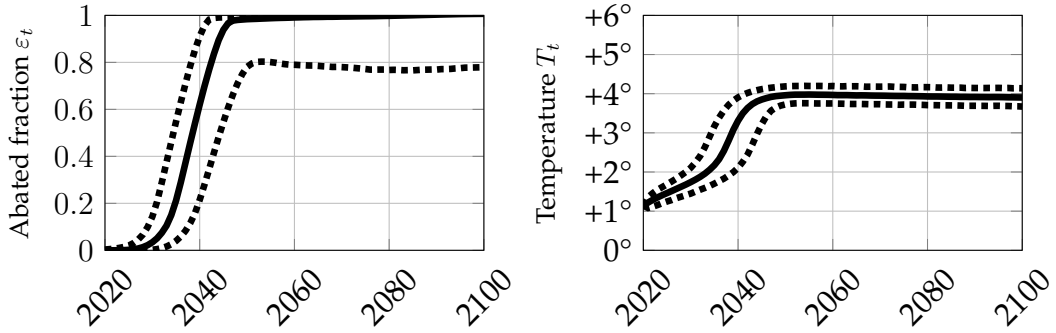

Figure 15: Median and 95% simulation intervals of the abated fraction of emissions ε_t (top left panel), the resulting expenditure in abatement as a % of output Y_t (top right panel), the temperature T_t (bottom left panel), and the carbon concentration (bottom right panel). Calculated from 10000 simulations using policy (33)

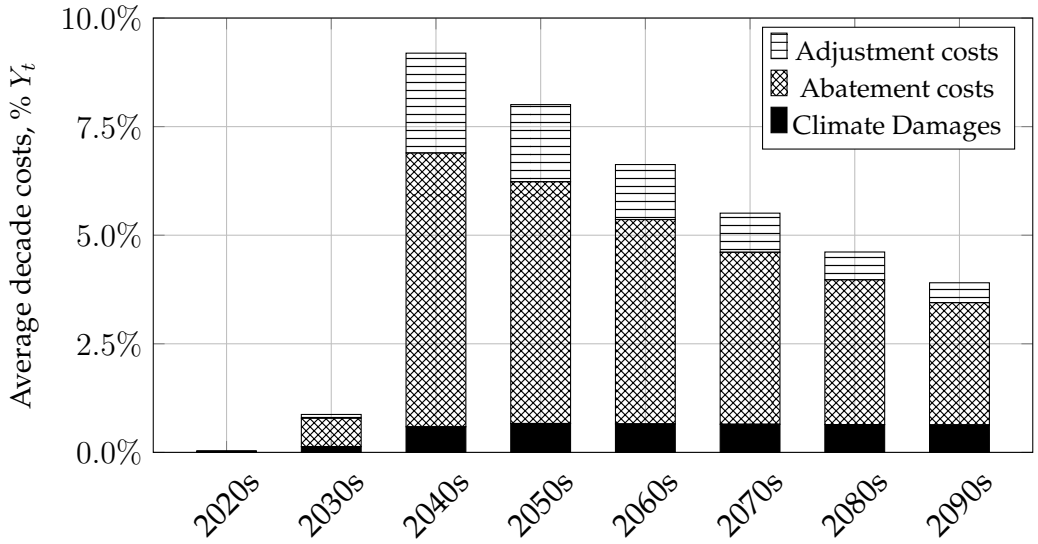

Figure 16

$$\alpha_t^p = \begin{cases} \underline{\alpha}_t & \text{if } t < \tau, \\ \overline{\alpha}_t & \text{if } t \geq \tau. \end{cases} \tag{34}$$

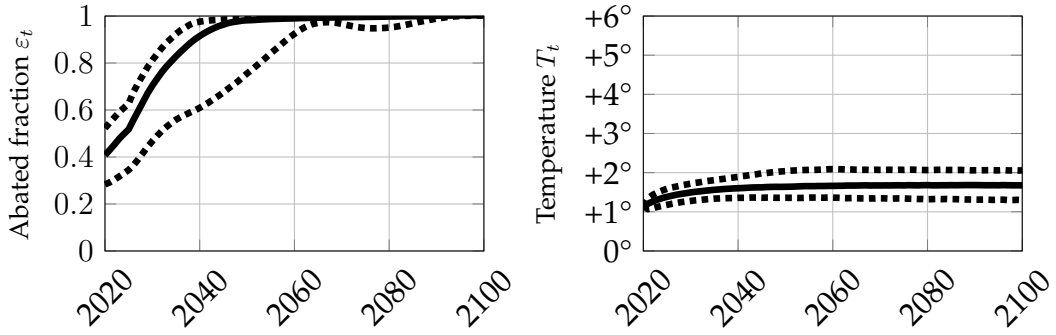

Figure 17: Median and 95% simulation intervals of the abated fraction of emissions ε_t (top left panel), the resulting expenditure in abatement as a % of output Y_t (top right panel), the temperature T_t (bottom left panel), and the carbon concentration (bottom right panel). Calculated from 10000 simulations using policy (34)

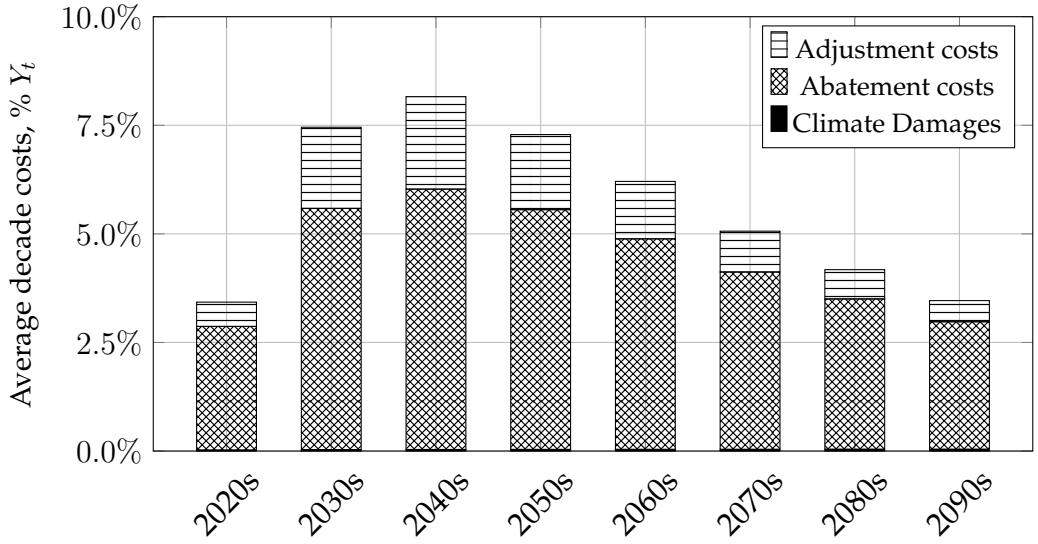

Figure 18

6 Conclusion

References

Ackerman, Frank, Elizabeth A. Stanton, and Ramón Bueno. 2013. "Epstein–Zin Utility in DICE: Is Risk Aversion Irrelevant to Climate Policy?" *Environmental and Resource Economics*, 56(1): 73–84. 39

Ashwin, Peter, Sebastian Wieczorek, Renato Vitolo, and Peter Cox. 2012. "Tipping Points in Open Systems: Bifurcation, Noise-Induced and Rate-Dependent Examples in the Climate System." *Philosophical Transactions of the Royal Society A: Mathematical, Physical and Engineering Sciences*, 370(1962): 1166–1184. 12

Baker, Erin, Leon Clarke, and Ekundayo Shittu. 2008. "Technical Change and the Marginal Cost of Abatement." *Energy Economics*, 30(6): 2799–2816. 20

Barro, Robert J. 2006. "On the Welfare Costs of Consumption Uncertainty." *National Bureau of Economic Research*, , (12763). 17

Ben-Yami, Maya, Andreas Morr, Sebastian Bathiany, and Niklas Boers. 2024. "Uncertainties Too Large to Predict Tipping Times of Major Earth System Components from Historical Data." *Science Advances*, 10(31): eadl4841. 2, 8, 13, 25

Boulton, Chris A., Lesley C. Allison, and Timothy M. Lenton. 2014. "Early Warning Signals of Atlantic Meridional Overturning Circulation Collapse in a Fully Coupled Climate Model." *Nature Communications*, 5(1): 5752–5752. 13

Cai, Yongyang, Timothy M. Lenton, and Thomas S. Lontzek. 2016. "Risk of Multiple Interacting Tipping Points Should Encourage Rapid CO2 Emission Reduction." *Nature Climate Change*, 6(5): 520–525. 4

Crost, Benjamin, and Christian P. Traeger. 2013. "Optimal Climate Policy: Uncertainty versus Monte Carlo." *Economics Letters*, 120(3): 552–558. 39

Dell, Melissa, Benjamin F Jones, and Benjamin A Olken. 2009. "Temperature and Income: Reconciling New Cross-Sectional and Panel Estimates." *American Economic Review*, 99(2): 198–204. 19

Dell, Melissa, Benjamin F Jones, and Benjamin A Olken. 2012. "Temperature Shocks and Economic Growth: Evidence from the Last Half Century." *American Economic Journal: Macroeconomics*, 4(3): 66–95. 19

Dietz, Simon, and Bruno Lanz. 2019. "Growth and Adaptation to Climate Change in the Long Run." IRENE Institute of Economic Research IRENE Working Papers 19-09. 19

Dietz, Simon, and Frank Venmans. 2019. "Cumulative Carbon Emissions and Economic Policy: In Search of General Principles." *Journal of Environmental Economics and Management*, 96: 108–129. 20

Dietz, Simon, Frederick Van Der Ploeg, Armon Rezai, and Frank Venmans. 2020. "Are Economists Getting Climate Dynamics Right and Does It Matter?" *SSRN Electronic Journal*. 4

Ditlevsen, Peter D., and Sigfus J. Johnsen. 2010. "Tipping Points: Early Warning and Wishful Thinking." *Geophysical Research Letters*, 37(19): 2010GL044486. 13

Duffie, Darrell, and Larry G. Epstein. 1992. "Asset Pricing with Stochastic Differential Utility." *Review of Financial Studies*, 5(3): 411–436. 22

Epstein, Larry G., and Stanley E. Zin. 1989. "Substitution, Risk Aversion, and the Temporal Behavior of Consumption and Asset Returns: A Theoretical Framework." *Econometrica*, 57(4): 937. 38

Ghil, Michael, and Stephen Childress. 2012. *Topics in Geophysical Fluid Dynamics: Atmospheric Dynamics, Dynamo Theory, and Climate Dynamics*. Vol. 60, Springer Science & Business Media. 12

Greiner, Alfred, and Willi Semmler. 2005. "Economic Growth and Global Warming: A Model of Multiple Equilibria and Thresholds." *Journal of Economic Behavior & Organization*, 57(4): 430–447. 4

Hambel, Christoph, Holger Kraft, and Eduardo Schwartz. 2021. "Optimal Carbon Abatement in a Stochastic Equilibrium Model with Climate Change." *European Economic Review*, 132: 103642. 3, 4, 5, 9, 17, 19, 22, 34, 40, 41

IPCC. 2023. *Climate Change 2021 – The Physical Science Basis: Working Group I Contribution to the Sixth Assessment Report of the Intergovernmental Panel on Climate Change.* . 1 ed., Cambridge University Press. 13, 17, 20

Kamien, Morton I., and Nancy L. Schwartz. 1971. "Sufficient Conditions in Optimal Control Theory." *Journal of Economic Theory*, 3(2): 207–214. 4

Kriegler, Elmar, Nico Bauer, Alexander Popp, Florian Humpenöder, Marian Leimbach, Jessica Strefler, Lavinia Baumstark, Benjamin Leon Bodirsky, Jérôme Hilaire, David Klein, Ioanna Mouratiadou, Isabelle Weindl, Christoph Bertram, Jan-Philipp Dietrich, Gunnar Luderer, Michaja Pehl, Robert Pietzcker, Franziska Piontek, Hermann Lotze-Campen, Anne Biewald, Markus Bonsch, Anastasis Giannousakis, Ulrich Kreidenweis, Christoph Müller, Susanne Rolinski, Anselm Schultes, Jana Schwanitz, Miodrag Stevanovic, Katherine Calvin, Johannes Emmerling, Shinichiro Fujimori, and Ottmar Edenhofer. 2017. "Fossil-Fueled Development (SSP5): An Energy and Resource Intensive Scenario for the 21st Century." *Global Environmental Change*, 42: 297–315. 10

Kuik, Onno, Luke Brander, and Richard S.J. Tol. 2009. "Marginal Abatement Costs of Greenhouse Gas Emissions: A Meta-Analysis." *Energy Policy*, 37(4): 1395–1403. 20

Kushner, Harold J., and Paul Dupuis. 2001. *Numerical Methods for Stochastic Control Problems in Continuous Time.* Vol. 24 of *Stochastic Modelling and Applied Probability*, New York, NY:Springer New York. 36, 38

Lemoine, Derek, and Christian P. Traeger. 2016. "Ambiguous Tipping Points." *Journal of Economic Behavior & Organization*, 132: 5–18. 4, 17

Lemoine, Derek, and Christian Traeger. 2014. "Watch Your Step: Optimal Policy in a Tipping Climate." *American Economic Journal: Economic Policy*, 6(1): 137–166. 4

Li, Chuan-Zhong, Anne-Sophie Crépin, and Therese Lindahl. 2024. "The Economics of Tipping Points: Some Recent Modeling and Experimental Advances." *International Review of Environmental and Resource Economics*, 18(4): 385–442. 4, 17

Lontzek, Thomas S., Yongyang Cai, Kenneth L. Judd, and Timothy M. Lenton. 2015. "Stochastic Integrated Assessment of Climate Tipping Points Indicates the Need for Strict Climate Policy." *Nature Climate Change*, 5(5): 441–444. 4, 39

Mäler, Karl-Göran, Anastasios Xepapadeas, and Aart de Zeeuw. 2003. "The Economics of Shallow Lakes." *Environmental and Resource Economics*, 26(4): 603–624. 4

McGuffie, Kendal, and Ann Henderson-Sellers. 2014. *The Climate Modelling Primer*. . 4. ed ed., Chicester:Wiley Blackwell. 12, 13

Nævdal, Eric, and Michael Oppenheimer. 2007. "The Economics of the Thermohaline Circulation—A Problem with Multiple Thresholds of Unknown Locations." *Resource and Energy Economics*, 29(4): 262–283. 4

Nordhaus, William. 2019. "Economics of the Disintegration of the Greenland Ice Sheet." *Proceedings of the National Academy of Sciences*, 116(25): 12261–12269. 4

Nordhaus, William D. 1992. "An Optimal Transition Path for Controlling Greenhouse Gases." *Science*, 258(5086): 1315–1319. 19, 20

Nordhaus, William D. 2014. "Estimates of the Social Cost of Carbon: Concepts and Results from the DICE-2013R Model and Alternative Approaches." *Journal of the Association of Environmental and Resource Economists*, 1(1): 273–312. 39

Nordhaus, William D. 2017. "Revisiting the Social Cost of Carbon." *Proceedings of the National Academy of Sciences of the United States of America*, 114(7): 1518–1523. 20

Pindyck, Robert S, and Neng Wang. 2013. "The Economic and Policy Consequences of Catastrophes." *American Economic Journal: Economic Policy*, 5(4): 306–339. 17, 22

Seaver Wang, A. Foster, E. A. Lenz, J. Kessler, J. Stroeve, L. Anderson, M. Turetsky, R. Betts, Sijia Zou, W. Liu, W. Boos, and Z. Hausfather. 2023. "Mechanisms and Impacts of Earth System Tipping Elements." *Reviews of Geophysics*. 2, 13

Skiba, A. K. 1978. "Optimal Growth with a Convex-Concave Production Function." *Econometrica*, 46(3): 527. 4

Tsur, Yacov, and Amos Zemel. 1996. "Accounting for Global Warming Risks: Resource Management under Event Uncertainty." *Journal of Economic Dynamics and Control*, 20(6-7): 1289–1305. 4

Van den Bremer, Ton S., and Frederick Van der Ploeg. 2021. "The Risk-Adjusted Carbon Price." *American Economic Review*, 111(9): 2782–2810. 4

Van Der Ploeg, Frederick, and Aart De Zeeuw. 2018. "Climate Tipping and Economic Growth: Precautionary Capital and the Price of Carbon." *Journal of the European Economic Association*, 16(5): 1577–1617. 4, 17

Van Westen, René M., Michael Kliphuis, and Henk A. Dijkstra. 2024. "Physics-Based Early Warning Signal Shows That AMOC Is on Tipping Course." *Science Advances*, 10(6): eadk1189. 13

Wagener, F. 2013. "Regime Shifts: Early Warnings." In *Encyclopedia of Energy, Natural Resource, and Environmental Economics*. 349–359. Elsevier. 4, 13

Wagener, Florian. 2015. "Economics of Environmental Regime Shifts." In *The Oxford Handbook of the Macroeconomics of Global Warming*. , ed. Lucas Bernard and Willi Semmler, 0. Oxford University Press. 4

Weitzman, Martin L. 2012. "GHG Targets as Insurance against Catastrophic Climate Damages." *Journal of Public Economic Theory*, 14(2): 221–244. 18, 19

Weitzman, Martin L. 2014. "Fat Tails and the Social Cost of Carbon." *American Economic Review*, 104(5): 544–546. 17

A Distribution of temperature

This section derives the steady state density of temperature given a fixed carbon concentration. The density is then use to calibrate the climate sensitivity and the initial conditions.

The Fokker-Planck equation for the density of temperature p_t is

$$\partial_T \left\{ \frac{\mu(T,m)}{\epsilon}\, p_t(T) + \frac{1}{2}\left(\frac{\sigma_T}{\epsilon}\right)^2 p_t'(T) \right\} = 0. \tag{35}$$

The steady state temperature $\overline{p}$ then satisfies the differential equation

$$\frac{\mu(T,m)}{\epsilon}\, \overline{p}(T) + \frac{1}{2}\left(\frac{\sigma_T}{\epsilon}\right)^2 \overline{p}'(T) = 0. \tag{36}$$

One can readily checked that this is solved by

$$\overline{p}(T) \propto \exp\left(-\frac{V(T,m)}{\sigma_T^2/2\epsilon^2}\right), \tag{37}$$

where

$$\begin{aligned} V(T,m) &\coloneqq g(m)T + \int r(T)\,\mathrm{d}T \\ &= g(m)T + S_0(1-\lambda_1)T - \frac{\eta}{5}T^5 + S_0\Delta\lambda \log(1+\exp(T-T_i)). \end{aligned} \tag{38}$$

B Solution to Maximisation

This appendix deals with the solution of the maximisation problem (30).

B.1 Simplifying Assumptions on the Decay Rate of Carbon

To reduce the state space, following Hambel, Kraft and Schwartz (2021), I make an assumption on the decay rate of carbon. The calibrated carbon decay δ_m, as a function of the carbon stored in sinks N_t, is illustrated in Figure 19. The

calibration assumes a functional form

$$\delta_m(N_t) = a_\delta e^{-\left(\frac{N_t - c_\delta}{b_\delta}\right)^2}, \tag{39}$$

for parameters $a_\delta, b_\delta, c_\delta$.

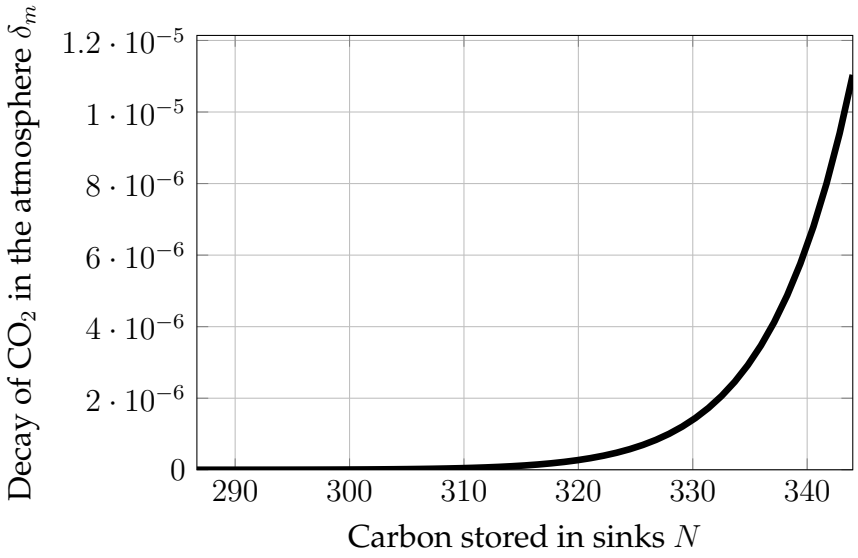

Figure 19: Estimated decay of carbon δ_m as a function of the carbon stored in sinks N_t.

I assume that the amount of carbon sinks present in the atmosphere is a constant fraction of the concentration in the atmosphere, $N_t = \frac{N_0}{M_0} M_t$. Abusing notation, I henceforth write $\delta_m(M_t)$ for the decay rate. Using this setup, under a business-as-usual emission scenario, the decay of carbon follows the path in Figure 20.

B.2 Hamilton-Jacobi-Bellman equation

Using the assumption from Appendix B.1, the value function V at time t depends only on temperature T_t, log-carbon concentration m_t and output Y_t. This

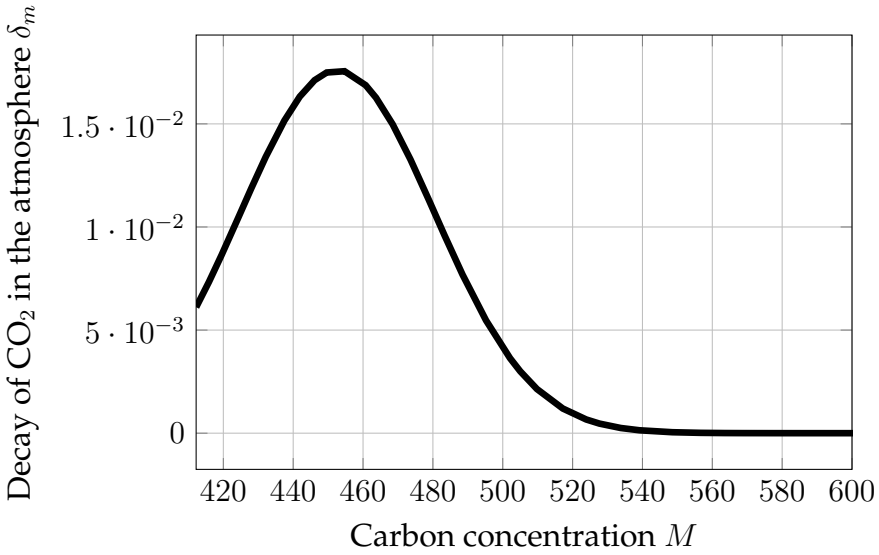

Figure 20: Estimated decay of carbon δ_m under the business as usual emission scenario M^b. Each marker is the decay after every decade.

satisfies the Hamilton-Jacobi-Bellman equation

$$\begin{aligned} -\partial_t V = \sup_{\chi,\alpha} & f(\chi Y, V) + \partial_m V\ (\gamma_t^b - \alpha) + \partial_m^2 V\ \frac{\sigma_m^2}{2} \\ & + \partial_Y V(\varrho + \phi(\chi) - d(T) - \beta_t(\varepsilon(\alpha))) + \partial_k^2 V\ \frac{\sigma_Y^2}{2} \\ & + \partial_T V\ \frac{r(T) + g(m)}{\epsilon} + \partial_T^2 V\ \frac{(\sigma_T/\epsilon)^2}{2}. \end{aligned} \tag{40}$$

It is easy to check that the ansatz

$$V_t(T, m, Y) = \frac{Y^{1-\theta}}{1-\theta} F_t(T, m) \tag{41}$$

satisfies (40).

B.3 Approximating Markov Chain

The Hamilton-Jacobi-Bellman equation (40) is solved for F by adapting the method proposed in Kushner and Dupuis (2001). The idea is to discretise the state space of T and m and compute time dependent intervals $\Delta t(T, m)$. Then, constructing a Markov chain $\mathcal{M}$ over the discretised space, parametrised by some small step size h. Then we compute a discretised value function F^h with

the property that $F^h \to F$ as $h \to 0$.

Given an h, construct a grid

$$\Omega_h = \{0, h, 2h, \ldots, 1-h, 1\}^2, \tag{42}$$

over the unit cube. This grid covers a suitable subset of the state space

$$\mathcal{X} \coloneqq [T^p, T^p + \Delta T] \times [m^p, m^p + \Delta m] \tag{43}$$

where Δm is chosen such that $T^p + \Delta T$ is stable at $m^p + \Delta m$.

Using the ansatz (41) we can define a discrete value function F_t^h over the grid such that $F_t^h \to F_t$ as $h \to 0$ over χ, that is

$$\begin{aligned} F_t^h(T_t, m_t) = \min_{\chi,\alpha} \Bigg(& \left(1 - e^{-\rho\Delta t}\right) \chi^{1-\frac{1}{\psi}} + \\ & e^{-\rho\Delta t} \left(\delta_y(\chi)\, \mathbb{E}_{t,\mathcal{M}(\alpha)} F_{t+\Delta t}^h(T_{t+\Delta t}, m_{t+\Delta t})\right)^{\frac{1-\frac{1}{\psi}}{1-\theta}} \Bigg)^{\frac{1-\theta}{1-\frac{1}{\psi}}} \end{aligned} \tag{44}$$

where

$$\begin{aligned} \delta_y(\chi) &\coloneqq \mathbb{E}_t \left[\left(\frac{Y_{t+\Delta t}}{Y_t} \right)^{1-\theta} \right] \\ &= 1 + \Delta t(1-\theta) \left(\varrho + \phi(\chi) - d(T_t) - \frac{\theta}{2}\sigma_k^2 \right) + \mathbb{E}_t\left[o(\Delta t^{\frac{3}{2}})\right]. \end{aligned} \tag{45}$$

and $\mathbb{E}_{t,\mathcal{M}(\alpha)}$ is the expectation with respect to the Markov chain $\mathcal{M}(\alpha)$ over the grid. This can be constructed, given a step size h, as follows. Introduce the normalising factor

$$Q_t(T, m, \alpha) \coloneqq \left(\frac{\sigma_T}{\epsilon \Delta T}\right)^2 + \left(\frac{\sigma_m}{\Delta m}\right)^2 + h \left| \frac{r(T) + g(m)}{\epsilon \Delta T} \right| + h \left| \frac{\gamma_t^b - \alpha}{\Delta m} \right|. \tag{46}$$

Then the probabilities of moving from a point (T, m) of the grid to an adjacent

point are given by

$$p(T \pm h\Delta T, m \mid T, m) \propto \frac{1}{2}\left(\frac{\sigma_T}{\epsilon \Delta T}\right)^2 + h\left(\frac{r(T) + g(m)}{\epsilon \Delta T}\right)^{\pm} \text{ and} \tag{47}$$

$$p(T, m \pm h\Delta m \mid T, m) \propto \frac{1}{2}\left(\frac{\sigma_m}{\Delta m}\right)^2 + h\left(\frac{\gamma_t^b - \alpha}{\Delta m}\right)^{\pm} \tag{48}$$

where $(\cdot)^+ \coloneqq \max\{\cdot, 0\}$ and $(\cdot)^- \coloneqq -\min\{\cdot, 0\}$. One can readily check that this is a well defined probability measure. Finally, the time step is given by

$$\Delta t = h^2 / Q_t(T, m, \alpha), \tag{49}$$

which satisfies $\Delta t \to 0$ as $h \to 0$.

Then, as the aggregator used in (44) converges to f (31) (Epstein and Zin, 1989), the chain described here satisfies the convergence properties outlined in Kushner and Dupuis (2001), we have $F_t^h \to F_t$ as $h \to 0$.

The Markov chain defined above allows to derive $F_t^h(T_t, m_t)$ from the subsequent $F_{t+\Delta t}^h(T_{t+\Delta t}, m_{t+\Delta t})$. This requires a terminal condition $\bar{F}^h(T_\tau, m_\tau) \coloneqq F_\tau^h(T_\tau, m_\tau)$. To derive this, assume that at some point in a far future $\tau \gg 0$, the abatement is free and all emissions are abated, $\gamma^b = \alpha$, such that $\mathrm{d}m = \sigma_m \, \mathrm{d}W_m$. Then we construct an equivalent, control independent, Markov chain $\bar{\mathcal{M}}$ as above for

$$\bar{F}^h(T_t, m_t) = \min_{\chi} \left(\left(1 - e^{-\rho \Delta t}\right) \chi^{1 - \frac{1}{\psi}} + e^{-\rho \Delta t} \left(\delta_y(\chi) \, \mathbb{E}_{t, \bar{\mathcal{M}}} \bar{F}^h(T_{t+\Delta t}, m_{t+\Delta t})\right)^{\frac{1-\frac{1}{\psi}}{1-\theta}} \right)^{\frac{1-\theta}{1-\frac{1}{\psi}}}. \tag{50}$$

This is now a fixed point equation for $\bar{F}$ which can be solved by value or policy function iteration.

C Calibration and Parameters

This section summarises the parameters for the preferences, economy, and climate model and discusses the calibration strategy.

The following Table 1 illustrates the preferences parameters used throughout the paper. There is no consensus in the literature on preference parameters. In line with previous literature focusing on recursive preferences, I set relative risk aversion $\theta = 10$ (Ackerman, Stanton and Bueno, 2013; Crost and Traeger, 2013; Lontzek et al., 2015) and the time preference parameter $\rho = 1.5\%$ (Nordhaus, 2014). There is no consensus on whether the elasticity of intertemporal substitution ψ ought to be larger or smaller than unity, with the aforementioned papers using values $\psi \in [0.75, 1.5]$. In this paper, I use $\psi = 1.5$ for the benchmark model and test the robustness of the results to $\psi = 0.75$.

Preferences		
ρ	1.5%	Time preference
θ	10	Relative risk aversion
ψ	1.5	Elasticity of intertemporal substitution

Table 1

Table 2 summarises the parameters of the economy model.

Economy		
ω_0	11%	GDP loss required to fully abate today
ω_r	2.7%	Rate of abatement cost reduction
ϱ	0.9%	Growth of TFP
κ	6.32%	Adjustment costs of abatement technology
δ_k	0.0116	Initial depreciation rate of capital
ξ	0.00026	Coefficient of damage function
ν	3.25	Exponent of damage function
A_0	0.113	Initial TFP
Y_0	75.8	Initial GDP
σ_k	0.0162	Variance of GDP
τ	500	Steady state horizon

Table 2

Table 3 summarises the parameters of the climate model.

Climate		
T_0	288.56 [K]	Initial temperature
T^{P}	287.15 [K]	Pre-industrial temperature
M_0	410 [p.p.m.]	Initial carbon concentration
M^{P}	280 [p.p.m.]	Pre-industrial carbon concentration
N_0	286.65543 [p.p.m.]	Initial carbon in sinks
σ_T	1.5844	Volatility of temperature
S_0	342 [W / m²]	Mean solar radiation
ϵ	15.844 [J / m² K year]	Heat capacity of the ocean
η	$5.67e-8$	Stefan-Boltzmann constant
G_1	20.5 [W / m²]	Effect of CO_2 on radiation budget
G_0	150 [W / m²]	Pre-industrial GHG radiation budget

Table 3

Non-linearity		
ΔT	1.8 [K]	temperature inflection point
λ_1	31%	Initial radiation reflected
$\Delta\lambda$	.	.

D Stochastic Tipping Benchmark Model

This appendix introduces a benchmark model with stochastic tipping. The stochastic tipping model is a widely used in the economic literature to approximate tipping points in the climate dynamics (e.g. Hambel, Kraft and Schwartz 2021). Comparing the model developed in this paper with the stochastic tipping model allows us to determine if and how the optimal abatement differ and, as a consequence, what the approximation misses.

To establish a meaningful benchmark, I will assume that the contribution of temperature to forcing (15) is given by

$$r_T^s(T) := S_0(1-\lambda_1) - \eta\sigma T^4. \tag{51}$$

This model has no tipping point as $\lambda(T) \equiv \lambda_1$. Stochastic tipping, as commonly modelled in the literature, is introduced as a jump process J with arrival rate $\pi(T)$ and intensity $\Theta(T)$, both increasing in temperature. Intuitively, as temperature rises, the risk of tipping $\pi(T)$ and the size of the temperature increase

$\Theta(T)$ grow. Then temperature dynamics in the Stochastic Tipping model follow

$$\epsilon \, \mathrm{d}T = \big(r^s(T) + g(m)\big) \, \mathrm{d}t + \sigma_x \, \mathrm{d}w^s + \Theta(T_t) \, \mathrm{d}N \, . \tag{52}$$

Following Hambel, Kraft and Schwartz (2021), the calibrated arrival rate and temperature increase are calibrated as

$$\pi(T) = -\frac{1}{4} + \frac{0.95}{1 + 2.8e^{-0.3325(T - T^{\mathrm{P}})}} \text{ and} \tag{53}$$

$$\Theta(T) = -0.0577 + 0.0568(T - T^{\mathrm{P}}) - 0.0029(T - T^{\mathrm{P}})^2. \tag{54}$$